THE JOURNAL OF BIOLOGICAL CHEMISTRY VOL. 280, NO. 43, pp. 35815–35821, October 28, 2005

Fully Metallated S134N Cu,Zn-Superoxide Dismutase Displays Abnormal Mobility and Intermolecular Contacts in Solution*[S]

Received for publication, June 17, 2005 Published, JBC Papers in Press, August 16, 2005, DOI 10.1074/jbc.M506637200

Lucia Banci[‡§¶], Ivano Bertini[‡§¶1], Nicola D'Amelio[‡2], Elena Gaggelli[‡‖], Elisa Libralesso[‡], Irena Matecko[‡3], Paola Turano[‡§], and Joan Selverstone Valentine[**]

From the [‡]Magnetic Resonance Center, University of Florence, Via Luigi Sacconi 6, 50019 Sesto Fiorentino, Italy, [§]Department of Chemistry, University of Florence, Via Della Lastruccia 5, 50019 Sesto Fiorentino, Italy, [¶]FiorGen Foundation, Via Luigi Sacconi 6, 50019 Sesto Fiorentino, Florence, Italy, [‖]Department of Chemistry, University of Siena, Via Aldo Moro, 53100 Siena, Italy, and [**]Department of Chemistry and Biochemistry, University of California Los Angeles, Los Angeles, California 90095-1569

S134N copper-zinc superoxide dismutase (SOD1) is one of the many mutant SOD1 proteins known to cause familial amyotrophic lateral sclerosis. Earlier studies demonstrated that partially metal-deficient S134N SOD1 crystallized in filament-like arrays with abnormal contacts between the individual protein molecules. Because protein aggregation is implicated in SOD1-linked familial amyotrophic lateral sclerosis, abnormal intermolecular interactions between mutant SOD1 proteins could be relevant to the mechanism of pathogenesis in the disease. We have therefore applied NMR methods to ascertain whether abnormal contacts also form between S134N SOD1 molecules in solution and whether Cys-6 or Cys-111 plays any role in the aggregation. Our studies demonstrate that the behavior of fully metallated S134N SOD1 is dramatically different from that of fully metallated wild type SOD1 with a region of subnanosecond mobility located close to the site of the mutation. Such a high degree of mobility is usually seen only in the apo form of wild type SOD1, because binding of zinc to the zinc site normally immobilizes that region. In addition, concentration-dependent chemical shift differences were observed for S134N SOD1 that were not observed for wild type SOD1, indicative of abnormal intermolecular contacts in solution. We have here also established that the two free cysteines (6 and 111) do not play a role in this behavior.

Over 100 different mutations in the superoxide dismutase 1(SOD1)[4] gene have been linked to the inherited form of amyotrophic lateral sclerosis (ALS), a fatal neurodegenerative disease characterized by progressive death of motor neurons and consequent paralysis. The individual mutations have been shown to exert their pathological effects by a gain of function mechanism, implying that the copper-zinc superoxide dismutase variant (Cu,Zn-SOD) expressed from the mutated gene has in some way become toxic. Recent evidence suggests that SOD1-linked ALS, like many other neurodegenerative diseases, is a protein misfolding disorder characterized by abnormal deposits of aggregated proteins in neural tissues (1–3). Implicated also in the toxicity of ALS-mutant SOD1 proteins are accelerated oxidative damage and inhibition of proteasome, chaperone, or mitochondrial function (2, 4, 5).

Relatively large, insoluble proteinaceous inclusions are observed in neural tissue in ALS and other neurodegenerative diseases, but it has been proposed that, rather than causing the disease, these deposits of aggregated protein may be formed as a part of a defensive mechanism to sequester misfolded and oligomerized protein when excessive amounts accumulate. More recently it has been suggested that the toxic species are smaller, high molecular weight oligomerized proteins formed from abnormal contacts of misfolded proteins resulting in protofibrils, pores, or other toxic species (6–10). High molecular weight forms of oligomerized mutant SOD1 have been observed in several studies using ALS-SOD1 transgenic mice (11–13).

Many of the ALS-linked Cu,Zn-SOD variant proteins have been expressed, purified, and characterized in an effort to identify properties that they hold in common that differ from the same properties of wild type Cu,Zn-SOD (5). These studies have revealed a wide variability in their biophysical and biochemical properties. Those of the Cu,Zn-SOD variant proteins with modifications far from the metal binding region have normal SOD activities and spectroscopic characteristics. Their three-dimensional crystal structures are overall quite similar to those of wild type Cu,Zn-SOD and thus give no clues as to possible mechanisms of misfolding and aggregation (14, 15). For that reason, it has been hypothesized that those mutant proteins may adopt a toxic form either prior to folding and metallation or subsequent to covalent modification or partial degradation (5, 16–19).

By contrast, the Cu,Zn-SOD variant proteins with modifications near the metal-binding sites, *i.e.* in either the zinc or the electrostatic loops, show altered SOD activities and spectroscopic properties. Some of them, specifically metal-deficient S134N and H46R SOD1, have been shown to crystallize in filament-like arrays with abnormal contacts between the individual protein dimers (20, 21). The presence of abnormal protein-protein contacts in the crystal structures of the ALS-linked Cu,Zn-SOD variant proteins suggests the possibility that similar intermolecular contacts may be made in solution in the earliest steps of the protein oligomerization that ultimately leads to aggregation.

In the current study, several spectroscopic techniques have been

* This work was supported in part by Ministero Italiano dell'Universita' e della Ricerca PRIN-2003, by European Union Contract LSHG-CT-2004-512052 "UPMAN-Understanding Protein Misfolding and Aggregation by NMR", and grants from the National Institute of General Medical Sciences (GM28222) and from the Amyotrophic Lateral Sclerosis Association (to J. S. V.). The costs of publication of this article were defrayed in part by the payment of page charges. This article must therefore be hereby marked "*advertisement*" in accordance with 18 U.S.C. Section 1734 solely to indicate this fact.

[S] The on-line version of this article (available at http://www.jbc.org) contains supplemental Fig. S1 and supplemental Tables S1 and S2.

[1] To whom correspondence should be addressed. Tel.: 39-055-4574272; Fax: 39-055-4574271; E-mail: ivanobertini@cerm.unifi.it.

[2] Recipient of a fellowship provided by Consorzio Interuniversitario per le Risonanze Magnetiche di Metalloproteine Paramagnetiche.

[3] Recipient of a Marie Curie host fellowship for early stage research training (contract MEST-CT-2004-504391 "NMR in Inorganic Structural Biology").

[4] The abbreviations used are: SOD, superoxide dismutase; *as*SOD, SOD in which Cys-6 and Cys-111 have been mutated to Ala and Ser, respectively; ALS, amyotrophic lateral sclerosis; HSQC, heteronuclear single quantum coherence; NMRD, nuclear magnetic relaxation dispersion; NOESY, nuclear Overhauser effect spectroscopy; R_1, longitudinal relaxation rate; R_2, transversal relaxation rate; TOCSY, total correlation spectroscopy; EPR, electron paramagnetic resonance.

applied to probe the structure and dynamics of the fully metallated S134N SOD1 protein in solution. Studies were carried out using both S134N *as*SOD1 and S134N *wt*SOD1. ("S134N *as*SOD1" or "*as*S134N" denotes a protein in which two additional mutations have been introduced, *i.e.* the 2 cysteine residues not involved in the intramolecular disulfide bond, Cys-6 and Cys-111, have been mutated to Ala and Ser, respectively. Those cysteines have not been removed in *wt*S134N or S134N *wt*SOD1). The former was used to ensure that any intermolecular contacts observed in solution were not due to formation of intermolecular disulfide bonds by air oxidation of the sample.

MATERIALS AND METHODS

Molecular Biology and Protein Characterization—The mutation S134N was introduced into *as*SOD1 by PCR mutagenesis, using the QuikChange® mutagenesis kit (Stratagene) and pPCuZnSODII^q as template. A plasmid encoding *wt*SOD1 and containing the same mutation was obtained by back mutation on pPCuZnSODII^q to get the *wt*SOD1 gene again and then inserting the mutation S134N as previously described. All the resulting constructs were sequenced to confirm the mutations. *Escherichia coli* TOPP1 strains were transformed with the obtained plasmids and with pPCuZnSODII^q.

To get large amounts of enzymes, the protein was expressed in 2xYT complex medium (22); to obtain uniformly ^{15}N- and, when needed, ^{13}C-labeled proteins for the sake of NMR studies, ^{15}N- and ^{13}C-enriched M9 chemically defined medium was used as described (23). An exception was the case of *wt*S134N, which was expressed without addition of copper sulfate to the culture because some expression tests revealed a sharp decrease in the protein yield upon addition of such salt. In the case of S134N *as*SOD1, the protein was isolated and purified as reported (24). Stock solutions of the proteins were stored at 4 °C, for short-term use, or at −20 °C. Further *in vitro* addition of Cu and Zn to the enzymes was not performed. Extraction and purification of S134N *wt*SOD1 followed the procedure of Hayward *et al.* (25) for insect cell cultures, adapted for use in *E. coli*.

Because the ^{15}N uniformly labeled *wt*S134N mutant showed lower solubility in ammonium sulfate than the unlabeled one, this specific enzyme was extracted from the cells using the same lysis buffer as the unlabeled one, but without NaCl, and was then purified by anionic exchange chromatography using the same protocol as for the *as*SOD1 mutants. In this case, 2 mM dithiothreitol was added to the elution buffers to keep the cysteines reduced during purification. Further *in vitro* addition of Cu and Zn was performed on the ^{15}N-labeled enzyme following a well known procedure (26) because it appeared to be largely in the apo form when checked by bidimensional NMR.

Metal content analysis of *wt*S134N and *as*S134N, obtained both from complex and chemically defined media, were performed using a Spectro Ciros charge-coupled device inductively coupled plasma optical emission spectrometer (Spectro Analytical Instruments) in combination with a Lichte nebulizer and a peristaltic pump for sample introduction. Concentrated stocks of proteins were diluted to a concentration of 3–5 μM in milliQ water. The inductively coupled plasma was programmed to detect three wavelengths for the Zn (202, 206, 213 nm) and three for the Cu (219, 219b, 324 nm), each measurement being repeated three times. The standardization curve was made using standard solutions in the range 0–10 μM Zn and Cu in milliQ water; a blank was also registered, using the protein buffer diluted in the same way as the samples themselves. Protein concentrations after dilution were determined using the Coomassie assay (Pierce Perbio) with bovine serum albumin as standard.

Spectroscopic Characterization—Spectra of S134N *as*SOD1 and S134N *wt*SOD1 were recorded both in the visible and in the UV range of wavelengths, using samples of concentration 10^{-4} M in the first case and diluting them 10-fold in the latter. The samples, in 20 mM phosphate buffer, pH 5, were centrifuged before performing the measurements.

Circular dichroism was used to characterize the secondary structure content of the mutants as well as the copper coordination environment. For the near-UV, spectra were collected on samples with concentrations ranging from 10 to 25 μM, at 298 K in the wavelength range 250–190 nm, on a Jasco J-810 spectrophotometer equipped with a Peltier unit. In the visible region spectra have been acquired on a 500-μM sample at 298 K in the wavelength 250–1000 nm, in 20 mM phosphate buffer at pH 5.

EPR spectra were recorded at 180 K on an Elexsys E500 spectrometer (Bruker), equipped with X-band microwave bridge (microwave frequency 9.45 GHz) and an ER 4131 VT unit for temperature control. 1-mM protein samples in 20 mM phosphate buffer at pH 5.0 were used.

NMRD measurements were performed on a set of 3 to 4 mM protein samples in 20 mM phosphate buffer, pH 5.0. Two distinct sets of measurements were performed, on the freshly prepared samples and on the same samples incubated at room temperature for a week, to promote oligomerization of the mutants. All measurements were made at a constant temperature of 298 K. To avoid the paramagnetic effect, reduction of Cu(II) to Cu(I) was achieved by addition of 1.2–1.5 equivalents of *p*-isoascorbic acid dissolved in degassed 20 mM phosphate buffer, pH 5, under reducing conditions. Longitudinal water proton relaxation rates were measured with a Stelar prototype of fast field cycling relaxometer (proton Larmor frequency 0.01–40 MHz). ^{1}H NMRD profiles were obtained by plotting water proton relaxation rates, after subtracting the relaxation rates of the buffer and normalizing the rates to 1 mM protein concentration, as a function of applied magnetic field.

High Field NMR—All the protein samples were in 20 mM phosphate buffer, pH 5.0, and the Cu(II) ion was reduced according to the procedure described above. The protein concentration (calculated according to the monomer) in the ^{15}N samples was in the range 1.0–1.5 mM, whereas in ^{13}C, ^{15}N samples were in the range 2.0–2.5 mM.

For mutant *as*S134N, several experiments were performed with the aim of achieving extensive spectra assignment: HNHA, HCCH-TOCSY, ^{13}C-HSQC-NOESY, and ^{15}N-HSQC-NOESY on a Bruker Avance 900 MHz and HNCOCA and HNCA at 500 MHz.

Mobility experiments were performed on both mutants using a Bruker 600-MHz spectrometer. For concentration- and time-dependent experiments, an 800 MHz spectrometer equipped with cryoprobe was used. For the purpose of hydrogen/deuterium exchange, a sample of *as*S134N was reduced as previously described; the *p*-isoascorbic acid was then discarded by using a Pd-10 column under a reducing atmosphere, and the enzyme was lyophilized at −50 °C and ~0.5 bar. The sample was resuspended in D_2O, and *p*-isoascorbic acid was again added. ^{1}H-^{15}N HSQC spectra were acquired every hour for a total of 72 h using a 900-MHz spectrometer equipped with a cryoprobe.

Structure Modeling—NOE cross-peaks in three-dimensional ^{15}N and ^{13}C NOESY-HSQC spectra were integrated for the region flanking the mutation (residues 120–140) and for residues spatially close in the solution structure of the non-mutated protein (residues 70–76, 43–46, 61–63, 85, 86). Volumes were converted into 691 upper distance limits for inter-proton distances with the program CALIBA (27). For the remaining part of the protein upper distances were evaluated by the solution structure and used as additional constraints. Some NOE cross-peaks regarding this part of the protein were integrated in order to calibrate the calculated distances in the region surrounding the muta-

tion. Structure calculations were performed using the program DYANA (28). Two hundred random conformers of one subunit were annealed using the above constraints in 10,000 steps. The final family was made up of 20 structures with the lowest values for the target function.

RESULTS

The S134N *as*SOD1 protein was isolated with two copper and two zinc ions (supplemental Table S1) as it has been seen previously for the *as*SOD1 in our expression system (24). It is in the dimeric form, as indicated by gel filtration measurements (data not shown) and as further confirmed by ^{15}N NMR relaxation data and field-dependent water relaxation rates on freshly prepared samples (see below).

The mutant was characterized at 298 K and pH 5 using freshly prepared protein samples. The copper(II) form was used for the electronic absorption, circular dichroism, and electron paramagnetic resonance spectra to take advantage of the spectroscopic features of this metal ion for the characterization of the metal-binding site, whereas the copper(I) form of the protein was used for NMR and NMRD characterization to avoid paramagnetic effects that would complicate the spectral analysis. These last two sets of data were used to monitor the structural and dynamic features of the protein. The experimental data on the two oxidation states of the protein were then analyzed to obtain a complete picture of the mutant.

The Copper-binding Site—The copper coordination environment is only slightly altered with respect to that of the *as*SOD1 protein. Indeed, the CD spectrum in the visible region is essentially superimposable on that of native SOD1, with a negative band at 13,200 cm^{-1} and a positive band at 16,600 cm^{-1} (29). The EPR spectrum (supplemental Fig. S1) is characterized by $g_{//} = 2.26$, $g_{\perp} = 2.06$, and $A_{//} = 154 \times 10^{-4}$ cm^{-1}, *i.e.* parameters very close to those of native SOD1 (29). However, at variance with the native protein, which possesses a rhombic spectrum, the spectrum of *as*S134N is essentially axial. Axial EPR spectra have been observed for some other SOD1 mutant proteins, not related to ALS (29), indicating a more tetragonal geometry for copper(II) bound in these mutants.

Structural and Dynamic Properties—The secondary β-structure is essentially conserved, as suggested by CD measurements in the far UV region. The ^{15}N-^{1}H HSQC spectra of the *as*S134N and *as*SOD1 proteins are substantially superimposable (Fig. 1*A*), with the exception of a few resonances. Meaningful shift differences between *as*SOD1 and the *as*S134N variant are clustered in the surroundings of the mutation as summarized in Fig. 1*B*, from which is it clear that residues 127–140 sense a different environment in the mutant. The chemical shift for residues 130–140 approaches those typical for isolated amino acids as for random coil polypeptides, and the $^{3}J_{HNHa}$ values are consistently in the range 4.6–7.2 Hz. The ^{1}H, ^{15}N, and ^{13}C resonance assignments for *as*S134N are reported in supplemental Table S2.

The differences in chemical shifts for the backbone amides in this protein area are accompanied by differences in the dynamic properties of residues in the same area, in particular for residues 129–137 (Fig. 2). ^{15}N relaxation rates of proteins and {^{1}H}-^{15}N heteronuclear NOEs are sensitive to the overall protein tumbling and to local motions either faster than the protein tumbling or much slower, *i.e.* in the range of tens of microseconds to milliseconds that is typical of conformational equilibria. In the present case, the average values for R_1, R_2, and NOE, if the 129–137 fragment is not considered, were 0.80 ± 0.10 s^{-1}, 25.8 ± 4.5 s^{-1}, and 0.78 ± 0.14, respectively, which are very close to those of the *as*SOD1 protein (30). R_1 rates for the 129–137 fragment are sensibly larger, with average values of 1.10 ± 0.10 s^{-1}. R_2 rates and heteronuclear NOEs decrease dramatically to values in the range 11–23 s^{-1} for R_2 and to values smaller than 0.55 for the NOE. The ^{15}N relaxation parameters were instead uniform along the entire sequence in the protein with the native amino acid in position 134. The present data therefore point at extensive mobility on the nanosecond time scale in the protein segment 129–137, where an Asn replaces the native Ser.

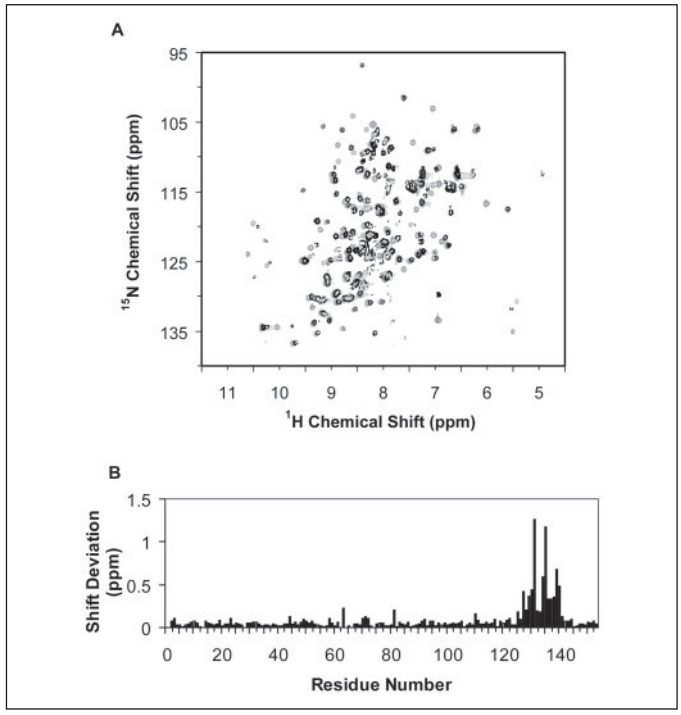

FIGURE 1. **^{15}N-HSQC superimposition of *as*SOD1 (*light gray*) and *as*S134N mutant (*black*) (*A*) and chemical shift deviations along the primary structure (*B*) computed as $((\Delta\delta_N^2/5+\Delta\delta_H^2)/2)^{1/2}$ where $\Delta\delta$ is the observed chemical shift change.**

The average rotational correlation time for a protein can in principle be estimated from the R_2/R_1 ratio. However, the ratio R_2/R_1 is also affected by the presence of conformational exchange and by motional anisotropy. On the other hand, the product R_1R_2 is independent of the overall correlation time and motional anisotropy and therefore can be used to highlight residues undergoing chemical exchange (31). A plot of R_1R_2 values for *as*S134N is shown in Fig. 2*D*, where an increase in the R_1R_2 values due to the presence of conformational exchange on the microsecond-millisecond time range is observed for a number of residues, consistent with the *as*SOD1 data (30). Additionally, reduced R_1R_2 values for residues 129–137 are observed, which further confirms the presence of fast motions for this protein fragment. From the ratio R_2/R_1, with the exclusion of residues involved in local fast motions or conformational exchange, an average correlation time for the protein tumbling of 18.1 ± 1.9 ns was estimated. Residues 129–137 experience an average correlation time of 12.3 ± 2.0 ns, which represents an estimate of the effective correlation time for the dipolar interactions in the 129–137 fragment.

The ^{1}H NMRD profiles report the water relaxation rates as a function of the magnetic field of millimolar solutions of protein and monitor the overall protein tumbling time. The profiles for the freshly prepared *as*S134N and *as*SOD1 are shown in Fig. 3, *A* and *B*. Their best fit was performed using the Model-free approach (32) (*solid line*), which provides an estimate of correlation time for the protein tumbling. For the *as*S134N variant this value is 20.0 ns and compares well with that of the *as*SOD1, for which a correlation time of 20.5 ns is calculated, thus clearly confirming that the mutant is also in the dimeric state. More-

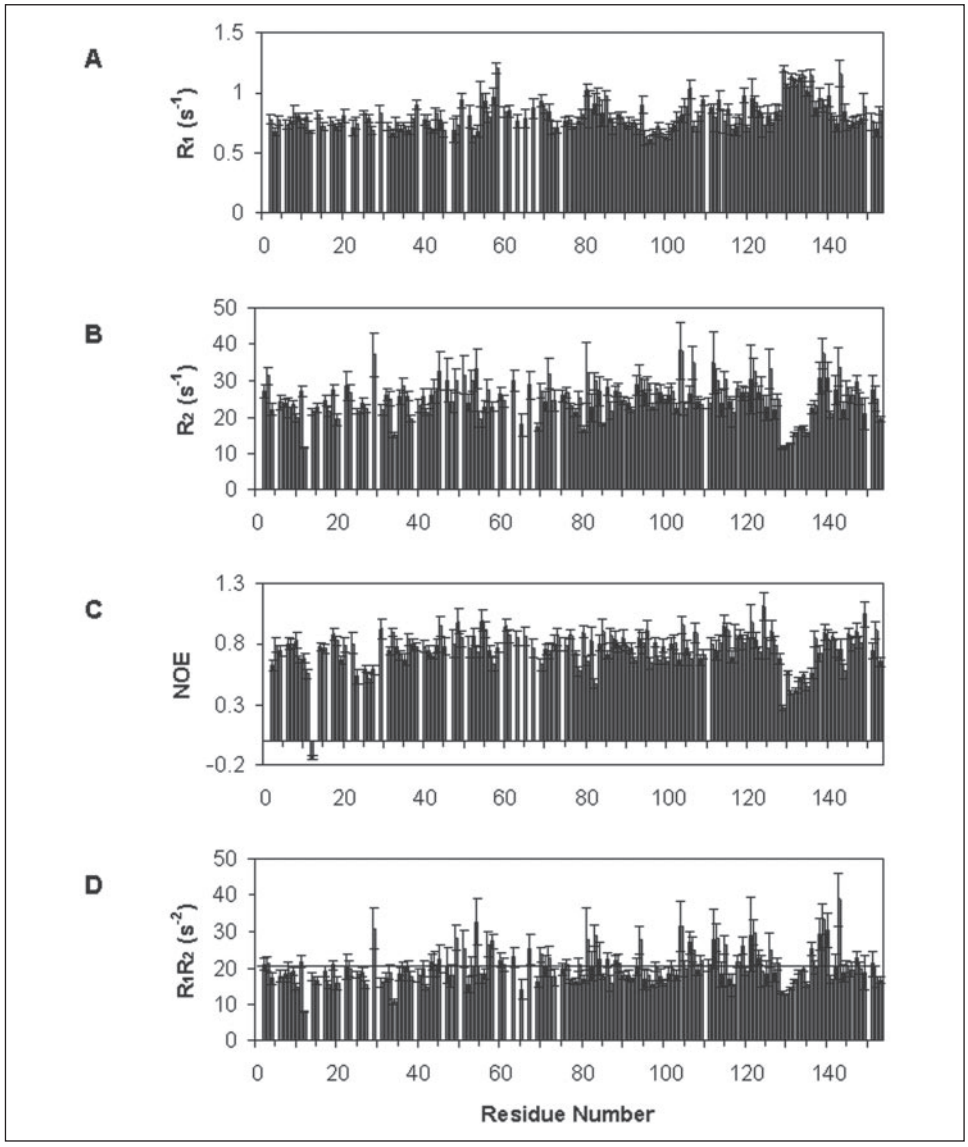

FIGURE 2. ^{15}N relaxation data (*A–C*) measured for S134N *as*SOD1. *D*, the values of the R_1R_2 product are reported for each residue; the *horizontal line* indicates the average value of R_1R_2 calculated excluding the mobile part of the protein around the mutation.

over, these correlation times are completely consistent with the values found from ^{15}N relaxation rates.

The time dependence of the hydrogen/deuterium exchange of backbone NH resonances provides information on their solvent accessibility. The per-residue exchange behavior of the *as*S134N mutant, as followed through ^{1}H-^{15}N HSQC spectra recorded every hour for 72 h after dissolving in D_2O a lyophilized sample of the protein, is similar to that of the *as*SOD1 studied under the same conditions (33) with the exception of the area surrounding the mutation. Indeed, in the *as*S134N variant, the backbone NHs of residues 127–143 are fully exchanged within the first hour, with residue 131 being completely exchanged within 2 h. In the case of the *as*SOD1, the residues in these areas exchange more slowly; complete exchange was reported to occur after ~6 h for Gly-129, Asn-131, and Thr-133 and after more than 12 h for Ser-134 and Lys-136 (33). Faster exchange in the variant in the area of the mutation is consistent with the presence of fast motions and lack of secondary structure, which make the backbone NHs more solvent accessible.

The number of NOEs/residue as measured from the ^{1}H-^{15}N HSQC-NOESY spectrum of *as*S134N mutant for the protein area around the mutation site is comparable with that observed for the native protein (33), although most of the NOEs are sensibly reduced in intensity. This effect is consistent with the presence of fast motions in this protein region as discussed above. Furthermore, the backbone sequential NOEs, as well as the $^{3}J_{HNH\alpha}$ and CSI values, do not indicate the presence of the short helix present in the native structure. Differences in long-range NOE patterns were not detected, except for a generic reduction in intensity that in some cases makes undetectable the NOEs that were already weak in *as*SOD1. In particular, the long-range NOEs between the 129–137 region characterized by fast internal motions and the protein fragment facing it in the structure of *as*SOD1 (residues 125–127) are weaker. However, these contacts are not lost, with the exception of those between the NH of Asp-125 and the side chain of residue 134 (the mutated residue). The introduction of a new residue slightly changed the NOE patterns for residue 134.

The structural model, calculated as described under "Materials and Methods," shows the region flanking the mutation quite disordered with backbone root mean square deviation values for the fragment 127–140 of 1.58 Å.

Tendency to Oligomerize—A macroscopic difference between the native protein and the *as*S134N mutant is the tendency of the latter to give rise to high molecular weight species in concentrated protein solutions. Such high molecular weight species are clearly observable as

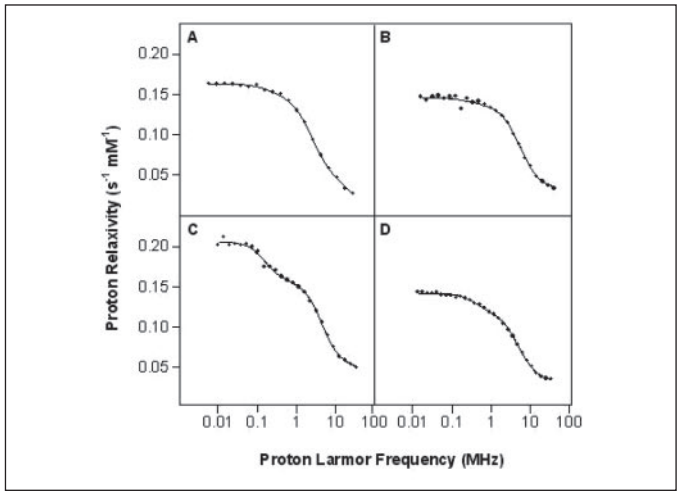

FIGURE 3. NMRD profiles of S134N *as*SOD1 freshly prepared (*A*) and after 3 weeks (*C*). Experiments were repeated for *as*SOD1 (*B* and *D*, respectively). The concentration of the protein samples was 3 mM at pH 5. Data were fitted using the Model-free approach (*solid line*). Fitting parameters were: *A*, $\alpha = 0.028\ s^{-1}$, $\beta = 6.7 \times 10^6\ s^{-2}$, $\tau = 20.0$ ns; *B*, $\alpha = 0.035\ s^{-1}$, $\beta = 5.4 \times 10^6\ s^{-2}$, $\tau = 20.5$ ns; *C*, $\alpha = 0.047\ s^{-1}$, $\beta = 5.8 \times 10^6\ s^{-2}$, $\tau_1 = 548$ ns, $\tau_2 = 19.0$ ns, $c_1 = 1.6$, $c_2 = 98.4$ (with c_i expressing the relative population of the two species with different molecular weight); *D*, $\alpha = 0.032\ s^{-1}$, $\beta = 5.0 \times 10^6\ s^{-2}$, $\tau = 21.6$ ns.

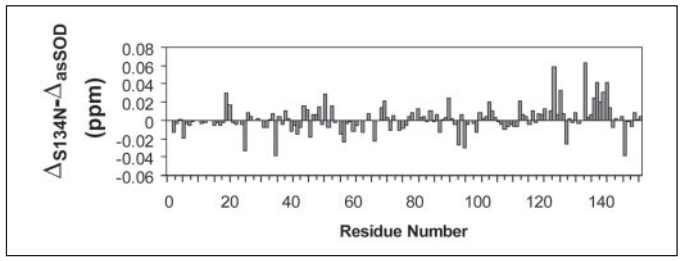

FIGURE 4. **Differences in chemical shift deviations between S134N *as*SOD1 and *as*SOD1 along the protein sequence, upon diluting the protein samples from 1.5 to 0.125 mM.** The chemical shift deviations are computed as $((\Delta\delta_N^2/5+\Delta\delta_H^2)/2)^{1/2}$ where $\Delta\delta$ is the observed chemical shift change.

insoluble entities in the NMR tube after a few days. The presence of large molecular weight protein forms was monitored through NMRD profiles. Although the freshly prepared protein has a profile very similar to that of the *as* form (Fig. 3, *A* and *B*), with time a new dispersion at lower field appears (Fig. 3*C*), indicating the presence of species with slow tumbling rates, *i.e.* of larger molecular weight. The relaxation dispersion profiles provide two independent correlation times, one as an average value for the large molecular weight species and one for the dimeric protein. For the latter a correlation time corresponding to that of the freshly prepared samples was obtained (19.0 ns). The extent of the oligomerization depends on protein concentration and time, but the dispersion at lower fields can always be interpreted as due to the presence of aggregates with molecular weight ~20–30 times larger than that of the dimeric protein. This effect does not have a counterpart in the *as* protein (Fig. 3*D*).

Another noticeable feature of the *as*S134N mutant is that the chemical shifts of residues around the mutation change depending on the sample concentration. By analyzing the chemical shift variations upon protein dilution for the *as*SOD1 and the S134N *as*SOD1 variants (stepwise dilution from 1.5 to 0.06 mM, followed at 800 MHz with a cryoprobe), some changes in chemical shift are observed for a number of residues. Nevertheless, a selective effect was detected in the S134N mutant for residues in the mutation area that does not correspond with the non-mutated protein under the same experimental conditions. The changes in chemical shift are larger at concentrations lower than 0.25 mM. The differences in chemical shift variation for the S134N *as*SOD1 and *as*SOD1 observed upon diluting the sample from 1.5 to 0.125 mM are reported in Fig. 4. The 0.125 mM was considered as final concentration because in the 0.06-mM sample some signal intensity was below the detection limit.

Removing the as Mutation—The results reported above describe the effect of the mutation in position 134 through the characterization of the mutated and non-mutated thermostable *as*SOD1 forms. It is clearly evident that the *as*S134N variant possesses a higher tendency toward aggregation although sharing with the non-mutated *as*SOD1 most of the structure and dynamics features; the main differences are limited to a very small protein fragment around the mutation site that becomes less structured and more flexible, with mobility faster than the overall tumbling.

The *wt*S134N is very similar to the *as*S134N, with essentially superimposable EPR spectra for the copper(II) and an electronic absorption spectrum with a maximum for the copper band at 655 nm. The differences in chemical shift observed through ^{15}N-^{1}H HSQC spectra in the protein area containing the mutation with respect to the *wt*SOD1 are reproduced also in the *wt*S134N derivative (data not shown). More importantly, the tendency toward aggregation is again displayed only by the *wt*S134N variant, thus proving that the effect of the S134N mutation is the same on the two *as* and *wt* protein scaffolds and does not depend on the presence of Cys-6 or Cys-111.

DISCUSSION

S134N *wt*SOD1 is partially metal deficient when isolated from its yeast or baculovirus expression systems and has been observed to crystallize in linear, amyloid-like filaments in which disorder in the loop regions has resulted in a deprotection of exposed β-strands and formation of abnormal intermolecular protein-protein contacts (20). These contacts are facilitated by the loss of zinc in the zinc site, which induces conformational heterogeneity in the zinc and electrostatic loops. Indeed, these loops are found to be significantly disordered in the x-ray structure, and residues 125–131 play an important role in filament formation as they participate to H-bonds and apolar interactions with the β-barrel of a neighboring protein molecule. This structure suggests that similar intermolecular contacts might be forming in solution as the first step in the protein oligomerization that leads to the toxicity associated with the disease.

We carried out the current study to determine the effect of the S134N mutation on the structure and dynamics of this region of the SOD1 protein and to look for evidence of abnormal intermolecular protein-protein contacts. We performed most of our studies on the S134N *as*SOD1 mutant in order to eliminate the possibility of aggregation due to formation of intermolecular disulfide bonds via Cys-6 or Cys-111. Comparative studies of S134N *as*SOD1 and S134N *wt*SOD1 confirmed that the *as* mutations had little, if any, effect on the structure and mobility of the proteins in solution. These results are in accord with numerous previous studies of *as*SOD1 mutants. The C6A and C111S mutations increase the thermostability of the sample, but they do not have discernible effects on the activity, structure, or mobility of SOD1. In particular, extensive data are available for the dimeric, fully metallated *as*SOD1 protein (33), for the monomeric, fully metallated *as*F50EG51EE133Q SOD1 derivative (30), for the apo (34) and copper-free states (35) of this monomeric form, and for the fully metallated familial amyotrophic lateral sclerosis-related mutant *as*G93A SOD1 (36).

Fully metallated *as*SOD1, $Cu(I)_2Zn_2$SOD, is a relatively rigid protein with rather uniform relaxation parameters (30). About 15 residues, 3 of which (residues 122, 126, and 129) are in the region of interest for the

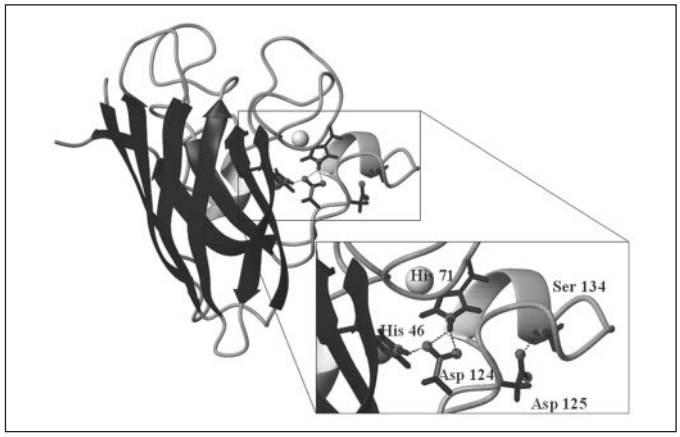

FIGURE 5. **H-bond network involving residues His-46, His-71, Asp-124, Asp-125, and Ser-134 in the wild type protein.** The figure has been generated from the x-ray crystal structure 1SOS (37). Zn and Cu ions are represented as spheres (*light* and *dark gray*, respectively).

present work, experience conformational exchange. The engineered monomeric protein in the fully metallated form behaves very similarly, with the exception of the area of loop IV where point mutations have been introduced to obtain the monomerization and which displays subnanosecond mobility (30).

The current study was carried out on fully metallated S134N proteins, and therefore the observed differences from the wild type protein can be attributed entirely to the mutation in position 134 and not to vacancies in metal-binding sites. We found here the behavior of fully metallated S134N *as*$Cu(I)_2Zn_2$SOD to be dramatically different from that of fully metallated *as*$Cu(I)_2Zn_2$SOD, either in the dimeric or the monomeric form. Indeed, we see high mobility in loop VII, comparable with that observed for apo-*as*SOD1, *despite the presence of zinc in the zinc site* in the *as*S134N variant. The absence of copper in monomeric zinc-only SOD derivative has previously been shown to have only limited effects on the structure and mobility of the *as*SOD1 protein, with slightly reduced order parameter values for the residues involved in copper binding (35). By contrast, in the monomeric apoprotein, where copper and zinc are both absent, loop IV (residues 45–85) and loop VII (residues 121–142) are largely unstructured and characterized by subnanosecond mobility, with $\{^1H\}$-^{15}N heteronuclear NOE and R_2 values sensibly smaller than the average and R_1 values larger than the average (34). Lack of zinc has, therefore, a destabilizing effect on loops IV and VII. We conclude that zinc binding to the zinc site of SOD1 normally causes a sequence of structural changes that results in a pinning of loop VII to the rest of the protein structure. The non-native structural plasticity of the fully metallated, familial amyotrophic lateral sclerosis-linked S134N mutant is a relevant difference with respect to the non-mutated *as* and *wt* proteins and might represent the key to understanding the peculiar behavior of this variant observed *in vitro*.

In the crystal structure of *as*SOD1, the native Ser-134 OH forms an H-bond with the carboxylate of Asp-125 (the distance between the donor oxygen and the acceptor oxygen being of the order of 2.7 Å), as shown in Fig. 5 (37). This H-bond belongs to an extensive H-bond network that also involves Asp-124 carboxylate H-bonded to the NH of two histidines, His-46 that is a copper ligand, and His-71 that is a zinc ligand. Based on our results, the substitution of the native Ser-134 with an Asn destabilizes this H-bond network in such a way that the presence of zinc is no longer sufficient to pin the electrostatic loop down, leaving it rather flexible. Consistent with this view, the major difference in the NOE patterns observed for the electrostatic loop (as discussed under "Results") concerns the loss of the dipolar connectivity between the NH of Asp-125 and the side chain of the amino acid in position 134. Moreover, the distances between the oxygen atoms of the carboxylate of Asp-125 and Nδ of Asn-134 are on average both longer than 4.5 Å in our model structure. Another hydrogen bond that is important in maintaining the conformation of the electrostatic loop in the non-mutated protein involves Asp-125 and Asn-139; this appears to be maintained in S134N protein.

In the crystal structure of metal-deficient S134N *wt*SOD1 (20), Leu-126 forms a small hydrophobic contact with Leu-42 of a neighboring SOD1 molecule. Leu-42 is located on a β structure and become deprotected upon mobilization of the zinc loop in the metal-deficient protein. A similar contact does not appear to be formed by fully metallated S134N in solution. However, in our solution model of the fully metallated *as*S134N, Leu-126 becomes more solvent exposed as a result of the S134N mutation. (The solvent accessible area goes from an average of 3.2% in the family of solution structures of *as*SOD1 to an average value of 9.7% in the family of the model structure of *as*S134N.) Meaningful chemical shift differences upon dilution are observed in the area around the mutation, and none of our data point to a possible involvement of Leu-42 in interprotein contacts in solution. We conclude, therefore, that the intermolecular protein-protein interaction does not involve that latter region in solution but is confined to the electrostatic loop.

Interestingly, abnormal contacts between different SOD1 molecules, similar to those described for the S134N derivative, are also observed in the crystal structure of the H46R familial amyotrophic lateral sclerosis-related variant (21) where the mutation site again involves a residue belonging to the above described H-bonding network.

It is quite clear from our results that the S134N variant, even in the fully metallated form, tends to generate protein oligomers. This finding implies that this derivative is prone to formation of intermolecular interactions. Protein surface areas characterized by fast mobility have been reported in the literature to be important for molecular recognition in macromolecular complexes (38), and a flexible area could also be important for protein-protein recognition between molecules of the same protein.

The observed concentration-dependent changes in chemical shift of S134N further support this picture. The change in resonance frequency is indicative of an altered structural environment consistent with an involvement of this protein area in weak intermolecular interactions that cannot be revealed by other means due to their transient nature. At micromolar protein concentrations, the chemical shifts probably reflect the situation in the absence of interactions, whereas at higher concentrations the interactions with other molecules affect the chemical shift. This could be a local effect, or it could be a selection of some of the possible protein conformations in these highly flexible regions upon interaction with other molecules.

In general, the observed chemical shift differences due to intermolecular interaction detectable by NMR are usually not large even when the protein-protein complex becomes the dominant species in solution (39). The fact that in the present SOD1 variant the observed variations in average chemical shift are smaller than 0.1 ppm and no indications of complex formation could be detected from the relaxation rates analysis implies that interactions among different SOD1 molecules involve very small amounts of the protein molecules in solution. However, such protein-protein interactions could represent a nucleation event that, once started, leads to quite large oligomers, no longer detectable by standard solution NMR but revealed in our NMRD studies. This latter process may provide insights at the molecular level into the early stages of the formation of the soluble oligomers or aggregates that have been proposed to be responsible for the protein toxicity.

Acknowledgment—We thank Dr. P. John Hart for helpful discussions.

REFERENCES

1. Bruijn, L. I., Houseweart, M. K., Kato, S., Anderson, K. L., Anderson, S. D., Ohama, E., Reaume, A. G., Scott, R. W., and Cleveland, D. W. (1998) *Science* **281,** 1851–1854
2. Bruijn, L. I., Miller, T. M., and Cleveland, D. W. (2004) *Annu. Rev. Neurosci.* **27,** 723–749
3. Rowland, L. P., and Shneider, N. A. (2001) *N. Eng. J. Med.* **344,** 1688–1700
4. Cleveland, D. W., and Rothstein, J. D. (2001) *Nat. Rev. Neurosci.* **2,** 806–819
5. Valentine, J. S., Doucette, P. A., and Potter, S. Z. (2005) *Annu. Rev. Biochem.* **76,** 563–569
6. Kirkitadze, M. D., Bitan, G., and Teplow, D. B. (2002) *J. Neurosci. Res.* **69,** 567–577
7. Sherman, M. Y., and Goldberg, A. L. (2001) *Neuron* **29,** 15–32
8. Lashuel, H. A., Hartley, D., Petre, B. M., Walz, T., and Lansbury, P. T. (2002) *Nature* **418,** 291
9. Morrison, B. M., Morrison, J. H., and Gordon, J. W. (1998) *J. Exp. Zool.* **282,** 32–47
10. Johnston, J. A., and Madura, K. (2004) *Prog. Neurobiol.* **73,** 227–257
11. Wang, J., Xu, G. L., Gonzales, V., Coonfield, M., Fromholt, D., Copeland, N. G., Jenkins, N. A., and Borchelt, D. R. (2002) *Neurobiol. Dis.* **10,** 128–138
12. Johnston, J. A., Dalton, M. J., Gurney, M. E., and Kopito, R. R. (2000) *Proc. Natl. Acad. Sci. U. S. A.* **97,** 12571–12576
13. Wang, J., Xu, G., and Borchelt, D. R. (2002) *Neurobiol. Dis.* **9,** 139–148
14. Hough, M. A., Grossmann, J. G., Antonyuk, S. V., Strange, R. W., Doucette, P. A., Rodriguez, J. A., Whitson, L. J., Hart, P. J., Hayward, L. J., Valentine, J. S., and Hasnain, S. S. (2004) *Proc. Natl. Acad. Sci. U. S. A.* **101,** 5976–5981
15. Hart, P. J., Liu, H., Pellegrini, M., Nersissian, A. M., Gralla, E. B., Valentine, J. S., and Eisenberg, D. (1998) *Protein Sci.* **7,** 545–555
16. Valentine, J. S., and Hart, P. J. (2003) *Proc. Natl. Acad. Sci. U. S. A.* 3617–3622
17. Lindberg, M. J., Tibell, L., and Oliveberg, M. (2002) *Proc. Natl. Acad. Sci. U. S. A.* **99,** 16607–16612
18. Arnesano, F., Banci, L., Bertini, I., Martinelli, M., Furukawa, Y., and O'Halloran, T. V. (2004) *J. Biol. Chem.* **279,** 47998–48003
19. Ray, S. S., Novak, R. J., Brown, R. H., Jr., and Lansbury, P. T., Jr. (2005) *Proc. Natl. Acad. Sci. U. S. A.* **102,** 3639–3644
20. Elam, J. S., Taylor, A. B., Strange, R., Antonyuk, S., Doucette, P. A., Rodriguez, J. A., Hasnain, S. S., Hayward, L. J., Valentine, J. S., Yeates, T. O., and Hart, P. J. (2003) *Nature Struct. Biol.* **10,** 461–467
21. Antonyuk, S., Elam, J. S., Hough, M. A., Strange, R. W., Doucette, P. A., Rodriguez, J. A., Hayward, L. J., Valentine, J. S., Hart, P. J., and Hasnain, S. S. (2005) *Protein Sci.* **14,** 1201–1213
22. Banci, L., Bertini, I., Chiu, C. Y., Mullenbach, G. T., and Viezzoli, M. S. (1995) *Eur. J. Biochem.* **234,** 855–860
23. Banci, L., Benedetto, M., Bertini, I., Del Conte, R., Piccioli, M., Richert, T., and Viezzoli, M. S. (1997) *Magn. Reson. Chem.* **35,** 845–853
24. Getzoff, E. D., Cabelli, D. E., Fisher, C. L., Parge, H. E., Viezzoli, M. S., Banci, L., and Hallewell, R. A. (1992) *Nature* **358,** 347–351
25. Hayward, L. J., Rodriguez, J. A., Kim, J. W., Tiwari, A., Goto, J. J., Cabelli, D. E., Valentine, J. S., and Brown, R. H., Jr. (2002) *J. Biol. Chem.* **277,** 15923–15931
26. Beem, K. M., Rich, W. E., and Rajagopalan, K. V. (1974) *J. Biol. Chem.* **249,** 7298–7305
27. Güntert, P., Braun, W., and Wüthrich, K. (1991) *J. Mol. Biol.* **217,** 517–530
28. Güntert, P., Mumenthaler, C., and Wüthrich, K. (1997) *J. Mol. Biol.* **273,** 283–298
29. Banci, L., Bertini, I., Cabelli, D. E., Hallewell, R. A., Tung, J. W., and Viezzoli, M. S. (1991) *Eur. J. Biochem.* **196,** 123–128
30. Banci, L., Bertini, I., Cramaro, F., Del Conte, R., Rosato, A., and Viezzoli, M. S. (2000) *Biochemistry* **39,** 9108–9118
31. Kneller, J. M., Lu, M., and Bracken, C. (2002) *J. Amer. Chem. Soc.* **124,** 1852–1853
32. Bertini, I., Fragai, M., Luchinat, C., and Parigi, G. (2000) *Magn. Reson. Chem.* **38,** 543–550
33. Banci, L., Bertini, I., Cramaro, F., Del Conte, R., and Viezzoli, M. S. (2002) *Eur. J. Biochem.* **269,** 1905–1915
34. Banci, L., Bertini, I., Cramaro, F., Del Conte, R., and Viezzoli, M. S. (2003) *Biochemistry* **42,** 9543–9553
35. Banci, L., Bertini, I., Cantini, F., D'Onofrio, M., and Viezzoli, M. S. (2002) *Protein Sci.* **11,** 2479–2492
36. Shipp, E., Cantini, F., Bertini, I., Valentine, J. S., and Banci, L. (2003) *Biochemistry* **42,** 1890–1899
37. Parge, H. E., Hallewell, R. A., and Tainer, J. A. (1992) *Proc. Natl. Acad. Sci. U. S. A.* **89,** 6109–6114
38. Dyson, H. J., and Wright, P. E. (2005) *Nat. Rev. Mol. Cell. Biol.* **6,** 197–208
39. Arnesano, F., Banci, L., Bertini, I., Cantini, F., Ciofi-Baffoni, S., Huffman, D. L., and O'Halloran, T. V. (2001) *J. Biol. Chem.* **276,** 41365–41376

Fully Metallated S134N Cu,Zn-Superoxide Dismutase Displays Abnormal Mobility and Intermolecular Contacts in Solution

Lucia Banci, Ivano Bertini, Nicola D'Amelio, Elena Gaggelli, Elisa Libralesso, Irena Matecko, Paola Turano and Joan Selverstone Valentine

J. Biol. Chem. 2005, 280:35815-35821.
doi: 10.1074/jbc.M506637200 originally published online August 16, 2005
